Rain-yield per flash calculated from TRMM PR and LIS data and its relationship to the contribution of tall convective rain

Yukari N. Takayabu[1]

Received 16 July 2006; revised 15 August 2006; accepted 17 August 2006; published 23 September 2006.

[1] Rain-yields per flash (RPF) over the entire tropics were calculated from 3 years of data collected by a Lightning Imaging Sensor (LIS) and a Precipitation Radar (PR) housed onboard the Tropical Rainfall Measuring Mission (TRMM) satellite. The results confirm that RPF is a reliable indicator of precipitation regimes, with a marked land–ocean contrast and intermediate values over monsoonal regions and continental oceans. Mean RPF values averaged over the entire TRMM region are 3.94×10^8 kg fl^{-1} over land and 1.96×10^9 kg fl^{-1} over oceans. A good (-0.55) correlation between RPF and the Tall Convective Rain Contribution with a threshold of -20degC (TCRC$-$20C) was found especially over land. This result indicates that large amounts of tall convective rain are fundamentally associated with intense updrafts that are able to sustain vigorous lightning activity. The correlation is weaker over ocean, except for that over continental oceans. **Citation:** Takayabu, Y. N. (2006), Rain-yield per flash calculated from TRMM PR and LIS data and its relationship to the contribution of tall convective rain, *Geophys. Res. Lett.*, *33*, L18705, doi:10.1029/2006GL027531.

1. Introduction

[2] Previous studies note that tropical continental rain dominates tropical oceanic rain by a large margin in terms of convective intensity and lightning activity, even though comparative amounts of rain are observed over tropical oceanic convergence zones [e.g., *Zipser and Lutz*, 1994]. The concept of the Rain-yields per flash (RPF) was first introduced by *Williams et al.* [1992] as 'rainyields,' which is the amount of rain divided by the lightning frequency over a given period and area. They showed that RPF values for areas over land during Austral monsoonal wet seasons are significantly larger than those during the break periods. *Zipser* [1994] examined variations of similar parameter rain-thunderstorm ratio (RTR) but in monthly rain per monthly thunderstorm days during the Global Atmospheric Research Program Atlantic Tropical Experiment (GATE). He showed that RTR values for areas over ocean are substantially larger than those for areas over land, and proposed RTR as an index of continentality of convective rainfall. *Petersen and Rutledge* [1998, hereafter referred to as PR98] utilized global Optical Transient Detector (OTD) data to calculate RPF in various regions and seasons and obtained values of 4×10^8 kg fl^{-1} as typical continental values and $1-2 \times 10^{10}$ kg fl^{-1} as typical tropical oceanic values. Note that they used only cloud-to-ground flash numbers for RPF calculations in PR98, which may cause factor 2–3 differences from RPF values calculated with the total flash numbers.

[3] In terms of the mechanism of lightning electric charges, *Takahashi* [1978, 1984] demonstrated that the coexistence of snow, graupels, and supercooled water is essential for electrical charging. He suggested that cloud systems should have vigorous microphysical processes between the -30degC and -10degC levels. Recently, *Petersen and Rutledge* [2001] utilized TRMM PR precipitation profile data to show that lightning activity is related to the height of the precipitation. The authors documented a strong correlation between the estimated ice water content and lightning frequency, which was further confirmed globally by *Petersen et al.* [2005].

[4] Some studies [e.g., *Rosenfeld and Woodley*, 2003] emphasized the effects of aerosol on lightning activity. They proposed that greater amounts of aerosol injection act to decrease precipitation efficiency, increase cloud height, and activate lightning. However, another study presented counterexamples that involve no distinction in electrical parameters between completely different environmental conditions in terms of cloud condensation nuclei concentrations over the Amazon region [*Williams et al.*, 2002]. More recently, *Sherwood et al.* [2006] utilized AVHRR 3.7 um and 11 um data and TRMM LIS data for different seasons to describe a relationship between smaller particle size at high cloud-tops and increased lightning frequency. This finding seems to support the proposed CCN effects of aerosols on lightning activity; however, the pattern of correspondence between cloud particle size and lightning is not always convincing. On the other hand, a series of studies [e.g., *LeMone and Zipser*, 1980; *Jorgensen and LeMone*, 1989; *Zipser*, 1994, 2003; *Zipser and Lutz*, 1994] has indicated that atmospheric stratification is largely responsible for the vigorous convection required to activate lightning. *Petersen et al.* [1996] also showed a strong correlation between atmospheric instability and lightning over the tropical western Pacific Ocean. In summary, the origin of the precipitation regime change remains a controversial topic.

[5] The purpose of the present study is to depict the global distribution of RPF from TRMM PR and LIS data, in order to examine the utility of this value as an indicator of rain regimes. We also compare the RPF values with information on precipitation height to determine the physical information conveyed by RPF values.

2. Data and Methods

[6] We focus on three parameters derived from TRMM LIS and PR observations. The first parameter is RPF, which is the rainfall amount (in kg) divided by the number of

[1]Center for Climate System Research, the University of Tokyo, Kashiwa, Japan, and Japan Agency for Marine-Earth Science and Technology, Yokosuka, Japan.

0094-8276/06/2006GL027531

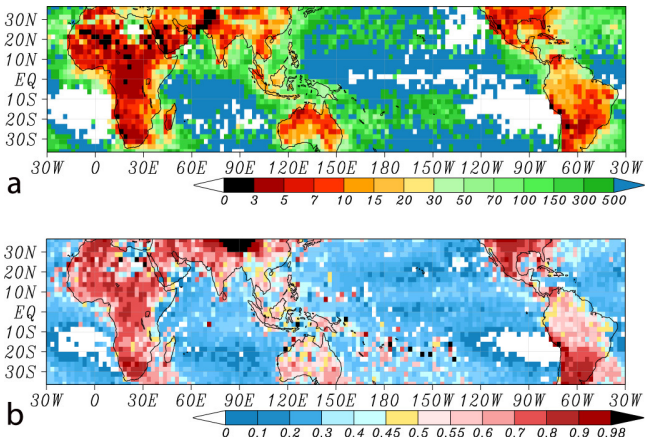

Figure 1. Global distributions of 3-year (March 1998–February 2001) (a) mean Rain-yields per flash and (b) Tall Convective Rain Contribution to surface rain with a threshold of −20degC. Units for the color scales are 10^7 kg fl^{-1} (Figure 1a) and fraction contribution (0–1) (Figure 1b). RPF averages are obtained by dividing the total precipitation amount by the total flash number for the averaging period.

lightning flashes observed over a given area and period. In calculating RPF, the TRMM satellite has the advantage of carrying both precipitation-measuring instruments and a lightning detector. Therefore, despite the fact that sampling error is a major concern in terms of orbiting satellite data, we can assume at the very least that we are observing close sampling areas for both precipitation and lightning data. For precipitation amount, we utilized the Precipitation Radar (PR)-based rainfall amount obtained from the daily TRMM 3G68 ver. 6 data for every 0.5 deg × 0.5 deg grid area. We obtained the lightning flash rate from TRMM LIS data using the OTD/LIS datasets prepared by *Boccippio et al.* [1998]. Although the swath width of PR is ∼215 km and the field of view of LIS is about 550 km × 550 km, we used all the LIS observation in order to maintain as large sampling area as possible for the lightning. In calculating RPF, we normalized both rain and flash number data for unit area and unit time. Both datasets are accumulated every 3 months to ensure that the 46-day return period of the TRMM satellite does not result in inhomogeneous diurnal sampling.

[7] The second parameter is the Tall Convective Rain Contribution to surface rain (TCRC; in %), with a threshold of −20degC. TCRC is the ratio of the surface convective rain with precipitation top heights (PTH) greater than the threshold temperature level, compared with the total surface convective rain. TCRC was calculated from the PR2A25 ver.5 dataset with the temperature data obtained from the 40-year Re-Analysis prepared by the European Centre for Medium-Range Weather Forecasts (ERA-40). The precipitation top was determined using a threshold of 0.3 mm hr^{-1}, which corresponds to the effective reflectivity factor (Ze) of ∼14 dBZ, with the rain-certain flag on, as used by *Takayabu* [2002]. Note that PTH is usually a few km lower than the cloud top height.

[8] The third parameter of interest is the Contribution to the Surface rain From Each Rain-top height (CSurFER; in mm hr^{-1}) derived from PR precipitation profiles for convective rain and stratiform rain, separately.

3. Results

[9] Figure 1a shows the global distribution of 3-year mean RPF values for the period from March 1998 to February 2001. The plot reveals a significant contrast in RPF over land and ocean, with smaller values being observed over land, typically less than 1.5–2.0 × 10^8 kg fl^{-1} (orange to reddish colors). Smaller RPF values are characterized by more vigorous lightning activity for the same amount of rain, while they are in opposite sense for larger RPF. The average RPF over land in the TRMM observation area of 36N–36S, 0–360E is 3.94 × 10^8 kg fl^{-1}, which corresponds well with the previous estimate by PR98, despite the differences in measurement methods. The average RPF over ocean within the TRMM observation area is 1.96 × 10^9 kg fl^{-1}, which is an order of magnitude smaller than the PR98's estimate for the tropical ocean. This discrepancy partially arises probably because PR98 estimated RPF over the warm pool region and our value is obtained from the entire tropical ocean average, and partially due to the difference that total flash numbers were used here while only cloud-to-ground flash numbers were used in PR98.

[10] The second notable feature in Figure 1a is that relatively small RPF values (yellowish and light green colors) recorded over oceanic areas adjacent to continents (hereafter referred to as 'continental oceans'), which are more pronounced to the east of continents. Especially significant regions are found over oceans to the east of North America, east of South Africa around Madagascar, east of South America, and east of the Indian subcontinent. These areas of relatively small RPF (less than 5.0 × 10^8 kg fl^{-1}) extend more than 1000 km from the continental margins. Similar but less pronounced trends are also observed to the east of East Asia, east of Australia, and in areas surrounding the Maritime Continent.

[11] The smallest values (less than 1.0 × 10^8 kg fl^{-1}) over land are found in equatorial Africa, South Africa, the area from the Sahel through the Arabian Peninsula to the Middle East, those parts of North America north of 25N, and in South America around the La Plata River. In contrast, the Amazon Basin, which is one of the most rainiest continental regions, and most of the Maritime Continent region except for the northern part of Sumatra Island are characterized by comparatively large RPF values of 1.5–5.0 × 10^8 kg fl^{-1}, with the largest values recorded over Papua New Guinea. Relatively large values are also found in East Asia, western India, southern Australia, Africa's east coast, and the central part of southern Africa around Zambia and Zimbabwe. These regions of comparatively large RPF over land correspond to monsoon regions where precipitation is characterized by oceanic features, especially during monsoonal wet seasons [e.g., *Williams et al.*, 1992; PR98; *Petersen and Rutledge*, 2001].

[12] As previous studies [e.g., *Takahashi*, 1984] have suggested that vigorous convective clouds in the temperature range from −10degC to −30degC are required for intensive lightning activity, we compared the global distribution of the TCRC−20C (Figure 1b) with that of RPF (Figure 1a) averaged for the same period. A significant correlation

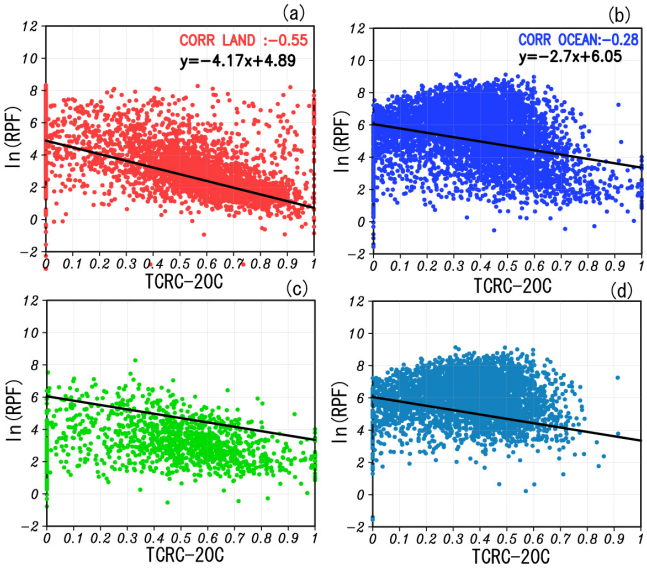

Figure 2. Scatter diagrams of ln(RPF) plotted against TCRC−20C for the tropical region of 20N−20S, 0−360E, for (a) areas over land, (b) areas over ocean, (c) areas over ocean but for those grids that 3 year-mean RPF is larger than 5.0×10^8 kg fl^{-1}, and (d) same as Figure 2c but for grids with 3 year-mean RPF $< 5.0 \times 10^8$ kg fl^{-1}. Black lines in Figures 2a and 2b are linear regression lines for each scatter plots, and those in Figures 2c and 2d are the same as the line in Figure 2b.

between the two variables is evident: small RPF values occur in areas where vigorous tall convective rain constitutes a large proportion of surface precipitation. TCRC greater than 70% is found in regions with small RPF values, whereas TCRC around 50% is found in monsoonal regions, and values are generally less than 40% over oceans. There are some exceptional regions where RPF and TCRC values do not coincide in the above manner, such as northern Australia, the Tibetan Plateau, Pakistan, and the southeastern coasts of the Arabian Peninsula. The reasons for these anomalies need to be considered in future studies.

[13] Figure 2 shows scatter diagrams of the seasonally averaged natural logarithm of RPF plotted against TCRC−20C. For these plots, seasonal mean values of RPF and TCRC over 2.5 deg × 2.5 deg grids were calculated separately for the March−May, June−August, September−November, and December−February seasons; these data were then utilized for the scatter plots and correlation analysis. The plots show a good negative correlation between the two variables, especially over land (Figure 2a), with a correlation coefficient of −0.55. The negative correlation over land is especially significant for TCRC−20C values above 0.3. No significant variation in RPF values is observed for TCRC−20C values less than 0.3. A negative correlation is also found for areas over ocean (Figure 2b), although with a much smaller correlation coefficient of −0.28. It is interesting to find that when we focus on the offshore transition zone by selecting the grids with 3 year-mean RPF values greater than 5.0×10^8 kg fl^{-1} which is mostly found around the continents (Figure 1a), the scatter plot (Figure 2c) shows very similar negative correlation to that observed for areas over land. On the other hand, when we plot for grids with the 3 year-mean RPF $< 5.0 \times 10^8$ kg fl^{-1}, mostly for open oceans, a greater scatter and a tendency of positive correlation for values of TCRC−20C less than 0.5 are observed. Therefore, it is confirmed that rain and thunderstorm characteristics in offshore transition zone over continental oceans is closer to those over land.

[14] Lastly, we examine rain profiles over ocean and over land using the average CSurFER for four zonal regions (Figure 3). For convective rain over land, a significant contribution from tall convective rain with PTH above 10 km, exceeding 0.05 mm day^{-1}, is observed in all four regions, while over ocean, the primary contribution is from rain with PTH below 9 km. We also observe a certain amount of contribution over ocean from rain with PTH below the freezing level. In areas over ocean in the deep tropics (20N to 20S), it is interesting that we find two peaks in CSurFER at PTH of ∼6.5 km and ∼9 km. For stratiform rain on the other hand, very similar profiles are found between over ocean and over land especially for the tropical region from 20N−20S, with twin contribution peaks at ∼7.5 km and ∼ 6 km. This land-ocean similarity in stratiform rain profiles is in contrast to the significant land-ocean difference in convective rain profiles. There is a third shallow stratiform peak at around 3 km, which is only observed over ocean. The above results indicate that while the characteristics of convective precipitation vary with changing environmental conditions, accompanying stratiform rain remains similar regardless of differences in environmental conditions. This is consistent with the findings of *Houze* [1989].

4. Discussion and Conclusions

[15] In this study, RPF values for the entire tropics were calculated from 3 years of TRMM LIS and PR data. The results indicate that RPF is a reliable indicator of precipitation

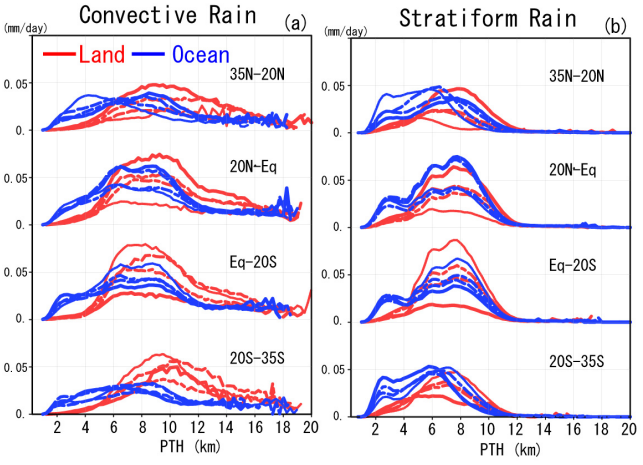

Figure 3. Contributions to the unconditional mean surface rain of rain columns at each precipitation-top height (PTH) in original 250 m bins, for (a) convective rain, and (b) stratiform rain for four zonal regions. Red lines indicate data over land and blue lines indicate those over ocean. Dash-dotted, solid, dashed, and dotted lines indicate the four seasons of March−May, June−August, September−November, and December−February, respectively.

regimes, with a marked land–ocean contrast and intermediate values over monsoonal regions and continental oceans. Mean RPF values averaged over the entire TRMM region are 3.94×10^8 kg fl^{-1} over land and 1.96×10^9 kg fl^{-1} over oceans. A good negative correlation (−0.55) exists between RPF and TCRC–20C, especially over land. This result indicates that large amounts of tall convective rain are fundamentally associated with intense convective updrafts that can sustain precipitation-sized particles in the supercooled water level and that result in vigorous lightning activity.

[16] In contrast, the overall correlation is weaker (−0.28) for RPF and TCRC–20C over ocean. In Figure 1a, we note that RPF values differ substantially between continental oceans and open oceans. Regional examinations of oceanic parameters (Figures 2c and 2d) indicate that the oceanic values show a higher-correlation relationship for continental oceans that resembles to the scatter plot over land, and a lower-correlation relationship for open oceans. Accordingly, for a given TCRC we observe larger RPF for open oceans than for continental oceans. One possible interpretation of this trend could be that aerosol-rich conditions over continental oceans results in greater numbers of continental-type clouds in such areas. A second explanation could involve the ubiquitous appearance of squall-line systems that are generated along-shore and propagate more than 1000 km from continental coasts. These systems have inherently continental characteristics with vigorous vertical velocity. Such systems are observed with distinct diurnal variations over the Borneo Sea [*Houze et al.*, 1981], the Bay of Bengal [*Zuidema*, 2003], the South China Sea [*Nitta and Sekine*, 1994; *Johnson et al.*, 2005], the area to the west of Sumatra Island [*Mapes et al.*, 2003; *Mori et al.*, 2004], and the area to the west of the Central American coast [*Mapes et al.*, 2003].

[17] We are currently undertaking detailed regional and seasonal analyses of RPF and precipitation profiles, including their diurnal variations. Direct comparisons of RPF and aerosol optical depth data recently retrieved from satellite measurements [e.g., *Rosenfeld*, 2006] may shed some light on the relationships between aerosol distribution and lightning activity. This task is left for future studies.

[18] **Acknowledgments.** The author is indebted to Tomoo Ushio for helping her with obtaining the TRMM LIS data. She also would like to acknowledge Steven C. Sherwood in Yale University and Walter A. Petersen in the University of Alabama-Huntsville for their helpful information on related topics. Stephen W. Nesbitt and an anonymous reviewer are gratefully acknowledged for their helpful review comments and suggestions. Thanks are extended to Chie Yokoyama for her collaboration with utilizing the LIS data. This study is supported by the Global Satellite Mapping of Precipitation (GSMaP) Project under the program Core Research for Evolutional Science and Technology (CREST) of the Japan Science and Technology Agency, and by the TRMM Fourth Japanese Research Announcement (TRMM JRA4) by the Japan Aerospace Exploration Agency.

References

Boccippio, D. J., K. Driscoll, J. Hall, and D. Buechler (1998), LIS/OTD Software Guide, 142 pp., Global Hydrol. and Clim. Cent., Huntsville, Ala.

Houze, R. A., Jr. (1989), Observed structure of mesoscale convective systems and implications for large-scale heating, *Q. J. R. Meteorol. Soc.*, *115*, 425–461.

Houze, R. A., Jr., S. G. Geotis, F. D. Marks Jr., and A. K. West (1981), Winter monsoon convection in the vicinity of North Borneo. Part I: Structure and time variation of the clouds and precipitation, *Mon. Weather Rev.*, *109*, 1595–1614.

Johnson, R. H., S. L. Aves, P. E. Ciesielski, and T. D. Keenan (2005), Organization of oceanic convection during the onset of the 1998 East Asian summer monsoon, *Mon. Weather Rev.*, *133*, 131–148.

Jorgensen, D. P., and M. A. LeMone (1989), Vertical velocity characteristics of oceanic convection, *J. Atmos. Sci.*, *46*, 621–640.

LeMone, M. A., and E. J. Zipser (1980), Cumulonimbus vertical velocity events in GATE, part I, diameter, intensity and mass flux, *J. Atmos., Sci.*, *37*, 2444–2457.

Mapes, B. E., T. T. Warner, and M. Xu (2003), Diurnal patterns of rainfall in northwestern South America. Part III: Diurnal gravity waves and nocturnal convection offshore, *Mon. Weather Rev.*, *131*, 830–844.

Mori, S., J. Hamada, Y. I. Tauhid, M. D. Yamanaka, N. Okamoto, F. Murata, N. Sakurai, H. Hashiguchi, and T. Sribmawati (2004), Diurnal land-sea rainfall peak migration over Sumatera Island, Indonesian Maritime Continent, observed by TRMM satellite and intensive rawinsonde soundings, *Mon. Weather Rev.*, *132*, 2021–2039.

Nitta, Ts., and S. Sekine (1994), Diurnal variation of convective activity over the tropical western Pacific, *J. Meteor. Soc. Japan*, *72*, 627–641.

Petersen, W. A., and S. A. Rutledge (1998), On the relationship between cloud-to-ground lightning and convective rainfall, *J. Geophys. Res.*, *13*(D12), 14,025–14,040.

Petersen, W. A., and S. A. Rutledge (2001), Regional variability in tropical convection: Observations from TRMM, *J. Clim.*, *14*, 3566–3586.

Petersen, W. A., S. A. Rutledge, and R. E. Orville (1996), Cloud-to-ground lightning observations from TOGA COARE: Selected results and lightning location algorithms, *Mon. Weather Rev.*, *124*, 602–620.

Petersen, W. A., H. J. Christian, and S. A. Rutledge (2005), TRMM observations of the global relationship between ice water content and lightning, *Geophys. Res. Lett.*, *32*, L14819, doi:10.1029/2005GL023236.

Rosenfeld, D. (2006), Aerosols, clouds, and climate, *Science*, *312*, 1323–1324.

Rosenfeld, D., and W. L. Woodley (2003), Spaceborne inferences of cloud microstructure and precipitation processes: synthesis, insights, and implications, *Meteorol. Monogr.*, *29*, 59–80.

Sherwood, S. C., V. T. J. Phillips, and J. S. Wettlaufer (2006), Small ice crystals and the climatology of lightning, *Geophys. Res. Lett.*, *33*, L05804, doi:10.1029/2005GL025242.

Takahashi, T. (1978), Riming electrification as a charge generation mechanism in thunderstorms, *J. Atmos. Sci.*, *35*, 1536–1548.

Takahashi, T. (1984), Thunderstorm electrification—A numerical study, *J. Atmos. Sci.*, *41*, 2541–2557.

Takayabu, Y. N. (2002), Spectral representation of rain profiles and diurnal variations observed with TRMM PR over the equatorial area, *Geophys. Res. Lett.*, *29*(12), 1584, doi:10.1029/2001GL014113.

Williams, E. R., S. A. Rutledge, S. G. Geotis, N. Renno, E. Rasmussen, and T. Rickenbach (1992), A radar and electrical study of tropical "hot towers", *J. Atmos. Sci.*, *49*, 1386–1395.

Williams, E. R., et al. (2002), Contrasting convective regimes over the Amazon: Implications for cloud electrification, *J. Geophys. Res.*, *107*(D20), 8082, doi:10.1029/2001JD000380.

Zipser, E. J. (1994), Deep cumulonimbus cloud systems in the tropics with and without lightning, *Mon. Weather Rev.*, *122*, 1837–1851.

Zipser, E. J. (2003), Some views on "hot towers" after 50 years of tropical field programs and two years of TRMM data, *Meteorol. Monogr.*, *29*, 49–58.

Zipser, E. J., and K. R. Lutz (1994), The vertical profile of radar reflectivity of convective cells—A strong indicator of storm intensity and lightning probability?, *Mon. Weather Rev.*, *122*, 1751–1759.

Zuidema, P. (2003), Convective clouds over the Bay of Bengal, *Mon. Weather Rev.*, *131*, 780–798.

Y. N. Takayabu, Center for Climate System Research, University of Tokyo, 5-1-5 Kashiwano-ha, Kashiwa, Chiba, 277-8568, Japan. (yukari@ccsr.u-tokyo.ac.jp)